OPTIMIZATION OF THE HEAT-ENGINEERING PROCESSES INVOLVING UTILIZATION OF CONTROL AND IDENTIFICATION METHODS

Yu. M. Matsevityi, A. V. Multanovskii, and I. A. Nemirovskii

UDC 536.24

We propose an economical algorithm for the identification of the thermal parameters and methods for the solution of the problem of optimizing heat-engineering systems.

In many technical systems one of the most important problems is that of the rapid cooling or heating of elements entering this system (the cooling of metallurgical production waste, the heating and cooling of heat-generation equipment when the latter is started up or shut down, etc.). Complexity in optimization and control of such systems can be ascribed to the multiplicity of components within such systems, in the laboriousness of mathematical simulation of such systems, as well as to the variety and frequent lack of formality in the limitations imposed on such systems. In this connection, it is very important correctly to formulate the problem, to select out of the great multiplicity of parameters those which affect the behavior of the system, and those which characterize the system from the standpoint of the process being studied, and from the standpoint of the formulated problem of optimization or control.

In this particular study we examine the problem that has arisen out of the requirements of metallurgical production, related to the change in the aggregate state of substances which take part in this technological process. The time required for the transition of the product into its final aggregate state determines to a great extent its quality and the productivity of the technological process. We will therefore solve the problem of optimization by resorting to approaches that are characteristic of the problems of optimum control for high-speed machinery, involving the identification of control signals, bringing the system to the desired state with optimum speed, and maximizing the quality of the selected criterion [1]. In order to solve the formulated problem it is necessary to choose a method for the identification of the control signals.

We studied the technological process of copper-melting slag granulation on a drum-type crystallizer which served simultaneously as a consumer of the slag heat. The granulation installation (Fig. 1) consists of two cooling drums 1, positioned underneath a slag discharge channel 2. The liquid slag 3 is crystallized at the surface of the rotating drums, forming a solid skin which is cut away by blades 4. The basic parameters affecting this technological process are the geometric dimensions of the surfaces of contact between the drum and the slag, the intensity of drum cooling, and the speed at which the drum rotates. Among the enumerated parameters, decisive is the speed of rotation, since the specific dimensions of each installation are specified, while the cooling intensity remains limited, i.e., limitations that are related to the cooling agent selected. The speed of drum rotation for the time of contact between the slag and the working surface thus become the unknowns in this problem of optimization. The magnitude of this velocity uniquely defines the thickness of the slag skin gelling in the crystallization process, i.e., we can speak of controlling the slag-hardening process. Figure 2 shows this process schematically, with the boundary Γ_{ph} (the dashed line) replacing the two-phase transition zone, since its thickness is smaller by two orders of magnitude than its length. The possibility of solving this problem in two-dimensional formulation is governed by the fact that the level and temperature of the melt along the generatrices of the cylindrical drum surfaces are identical, while the intensity with which the coolant removes heat is constant, i.e., the thermal pattern in any cross section perpendicular to the drum axes is unchanging.

Thus reducing this process to the Stefan problem, we nevertheless retain the temperature boundaries of the phase transition within the solution of the problem by replacing the average temperature $\overline{T}_{ph}$ of the phase transition by some quantity

$$\tilde{T}_{ph} = \overline{T}_{ph} \pm \Delta T_{ph} \tag{1}$$

where $\Delta T_{ph} = (T_\ell - T_s)/2$, T_ℓ and T_s are the liquidus and solidus temperatures (we will speak later upon the formation of $\tilde{T}_{ph}$ in connection with the utilization of the stochastic approach to the identification of control actions).

Institute for Problems in Machine Construction, Academy of Sciences of the Ukrainian SSR. Translated from Inzhenerno-Fizicheskii Zhurnal, Vol. 59, No. 2, pp. 298-308, August, 1990. Original article submitted April 11, 1989.

0022-0841/90/5902-1055$12.50

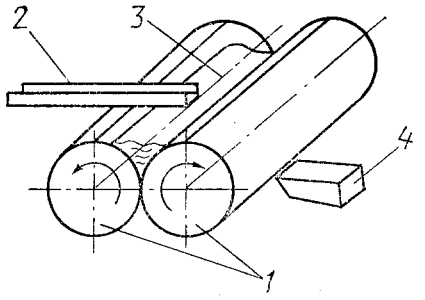

Fig. 1

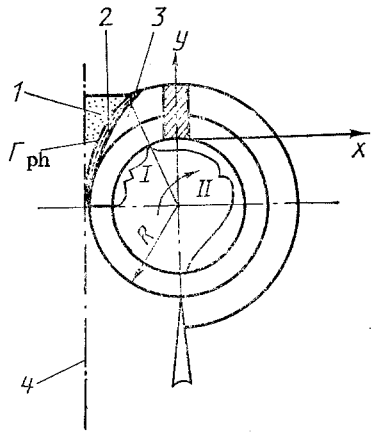

Fig. 2

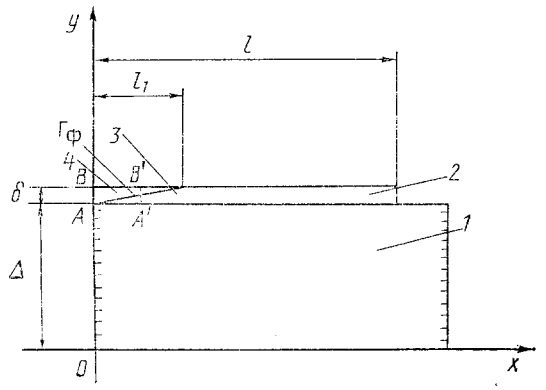

Fig. 3

Fig. 1. Slag granulation installation.

Fig. 2. Diagram of the slag granulation process: 1) liquid slag; 2) two-phase zone; 3) solid slag phase; 4) installation's axis of symmetry; Γ_{ph}) crystallization front in the Stefan problem.

Fig. 3. Model of the granulation process in Cartesian coordinates: 1) cooling drum; 2) solid slag phase in the aftercooling zone (stage II); 3) solid slag phase in the crystallization zone (stage I); 4) liquid slag phase; Γ_{ph}) crystallization front in the Stefan problem.

All of this pertains to zone I (Fig. 2), which corresponds to the first stage of the crystallization process. The second stage (after cooling) proceeds without any change in the aggregate state of the substance (zone II, Fig. 2) and is studied by means of an ordinary mathematical model of the phenomena of thermal conductivity for a solid. In this connection, the thermal processes in the first and second stages are examined separately.

On the basis of our studies and the recommendations from [2], it has been established that surface curvature affects the results from the solution of the thermal-conductivity problems only in the case of small drum diameters (less than 0.2 m). In the granulators being examined here, designed for large volumes of treated slags, the minimum drum diameters exceed 0.5 m, so that for both of the stages the concept of a granulation-process model in rectangular coordinates is permissible (Fig. 3). Replacement of the parabolic boundary of phase separation [3] by a straight line is equally valid for two reasons. First of all, the parabolic shape of the front of change in the aggregate state degenerates into a straight line, given a sufficiently large velocity of cooling-surface movements [2]. Second, such an assumption is possible with a slag-coating length many times greater than its thickness. This latter condition corresponds to intensive removal of heat, which is most effective in the cooling of thin slag layers [4].

Let us write the general mathematical model of the slag granulation process (for two stages):

$$\frac{\partial}{\partial x}\left[\lambda_{s}(T)\frac{\partial T}{\partial x}\right]+\frac{\partial}{\partial y}\left[\lambda_{s}(T)\frac{\partial T}{\partial y}\right]=c_{V_s}(T)\frac{\partial T}{\partial \tau}; \tag{2}$$

$$\frac{\partial}{\partial x}\left[\lambda_{d}(T)\frac{\partial T}{\partial x}\right]+\frac{\partial}{\partial y}\left[\lambda_{d}(T)\frac{\partial t}{\partial y}\right]=c_{V_d}(T)\frac{\partial T}{\partial \tau}; \tag{3}$$

$$-\lambda_{d}(T)\frac{\partial T}{\partial y}=\alpha_{c}(T-T_{c}); \tag{4}$$

$$\lambda_{s}(T)\frac{\partial T_s}{\partial y}=\lambda_{d}(T)\frac{\partial T_d}{\partial y};\quad T_s=T_d; \tag{5}$$

$$\lambda_{s.\ell}(T)\frac{\partial T}{\partial n}\Big|_{\Gamma_{ph}}=\lambda_{s.sol}(T)\frac{\partial T}{\partial n}\Big|_{\Gamma_{ph}}+\frac{L\rho_s(T)}{N}V(\tau): \tag{6}$$

$$-\lambda_{s}(T)\frac{\partial T}{\partial y}=\alpha_{a}(T-T_{a})+\varepsilon C_0\left[\left(\frac{T}{100}\right)^4-\left(\frac{T_a}{100}\right)^4\right]; \tag{7}$$

$$l_1<x\leqslant l; \tag{8}$$

$$T_p=T_{\ell};\quad 0<x\leqslant l_1;$$

$$T_p|_{x=0:\ \Delta\leqslant y\leqslant\Delta+\sigma}=T_{\ell}; \tag{9}$$

$$-\lambda_{s}(T)\frac{\partial T}{\partial x}\Big|_{\substack{x=l;\\ \Delta\leqslant y\leqslant\Delta+\delta}}=\alpha_a(T-T_a)+\varepsilon C_0\left[\left(\frac{T}{100}\right)^4-\left(\frac{T_a}{100}\right)^4\right]; \tag{10}$$

$$\lambda_{d}(T)\frac{\partial T}{\partial x}\Big|_{\substack{x=0\\ x=2\pi R;\ 0\leqslant y<\Delta}}=0, \tag{11}$$

where the thermal conductivity λ_s and the specific volumetric heat capacity c_{V_s} of the slag are equal to $\lambda_{s.sol}$, $c_{V_{s.sol}}$ when $T < T_{ph}$ and $\lambda_{s.\ell}$, $c_{V_{s.\ell}}$ when $T \geq T_{ph}$; λ_d, c_{V_d} is the thermal conductivity and specific heat capacity of the drum material; α_c is the coefficient of heat transfer from the wall of the drum to the coolant; $V(\tau)$ is the linear rate of hardening; N is the coefficient of crystallization intensification [2]; α_a is the coefficient of heat transfer from the slag to the air; ε is the emissivity; L is the latent heat of crystallization; T_c, T_a and T_ℓ are the temperatures of the coolant, air, and liquid slag; C_0 is the Stefan–Boltzmann constant; ℓ_1 is the length of the slag overflow zone (Fig. 3); δ is the thickness of the slag skin; Δ is the thickness of the drum wall. The intensification coefficient N, which takes into consideration the speed with which the cooling surface flows over into the crystallization layer, changes from 1 to 2 with an increase in the speed of drum motion from zero to a quantity corresponding to the maximum productivity. We can regard the contact between the slag and the drum as ideal [it is characterized by condition (5)], since the liquid slag adheres to the cooling surface of the drum. The productivity of the granulation installation can be raised to its maximum, at first glance, by increasing the thickness of the solidified slag skin that is removed from the drum, but in order to accomplish this it becomes necessary correspondingly to reduce the speed of drum rotation and this, naturally, will produce an opposite reaction. The greatest productivity can therefore be achieved by optimizing the thickness of the skin and the speed. The optimum speed will be determined by the time within which the slag skin passes through all stages of the process from the liquid phase to the solid, at a specified temperature. In other words, we have arrived at the problem of optimizing the thermal processes of crystallization (the first stage) and the aftercooling (second stage) of the slag.

Studies of the conduction of heat within the slag skin demonstrated that the flow of heat to the cooling agent in a direction parallel to the y axis (Fig. 3) is greater by 2-3 orders of magnitude than the flow in a direction parallel to the x axis. When we take this into consideration, as well as the relationship between the linear dimensions (the thickness of the hardening layer is smaller by 2-3 orders of magnitude than the characteristic dimensions of the cooling drum and the bath containing the liquid slag), it is a good idea to examine more closely the one-dimensional model of the heat system in which the temperature changes along the y axis, and the coordinate origin moves along the x axis (the boundary conditions, both above and below, change in this case in direct proportion to the movement of the system).

During the time required for the section under consideration to cover a path length ℓ_1 (the first stage) the crystallization front will be displaced through δ, i.e., the unknown time in our problem will be uniquely defined by the speed of motion for the boundary of phase separation. Since the outflow of heat in a direction parallel to the x axis nevertheless continues to exist and to some extent intensifies the transfer of heat and, consequently, accelerates the crystallization process, the true time of this process will not exceed that time determined for the one-dimensional model.

The adopted assumption with respect to the one-dimensionality of the temperature field in the slag skin, in principle, cannot be extended to the cooling drum. However, the need for a combined solution for the slag-drum system required that the problem for the drum also be reduced to a one-dimensional problem and that in order to account for additional heat transfer in the drum (in a direction parallel to the x axis) some effective thermal conductivity λ_{eff} be introduced in the place of λ_d.

In the formulated optimization problem the problem of choosing the reference (measured) values of the parameters and limitations appears rather complex. Studies have shown that in this system, particularly in the design stage, it is only the boundary of phase separation that can serve as the reference and (or) limiting factor. But when we resort to the terminology from control theory we can speak of a transition from the problem of optimum high-speed control to the problem of nonterminal control, when at any instant of time it is necessary to optimize the parameters of a system moving over a known trajectory $\tilde{T}_{ph} = f[x(\tau)]$ of transition from the original $T[x(\tau_0)]$ to the final $T[x(\tau_k)]$ state. Moreover, in this case we actually come to a problem of parametric identification since, in addition to $\tilde{T}_{ph}$, there are no other parameters defining the behavior of the system, and we have to find $V(\tau)$, i.e., the velocity of motion for the phase-separation boundary (the linear hardening rate). For the identification of $V(\tau)$ we have to solve the geometric reciprocal problem of heat conduction [5], for which the measurement equation has the following form:

$$(\tilde{T}_{ph})_k = Ah[V_k] + (\partial T_{ph})_k. \tag{12}$$

Here $\tilde{T}_{ph}$ is the temperature of the phase transition, whose velocity V_k of motion at each k-th instant of time is subject to identification; Ah[·] is the coupling operator for the estimated and "measured" parameter; the white Gaussian sequence ∂T_{ph} represents the error which takes into consideration ΔT_{ph} [see expression (1)] and the discrete nature of the three-dimensional model of the material being studied here (the drop in temperature across a series of units).

We propose the adaptive iteration filter for our identification method, since it has been modified for the identification of parameters in specialized computers (including limited-category computers). In its original form the iteration filter [5, 6] exhibits two fundamental shortcomings. First of all, precise knowledge of the transition matrices of the system is essential for its utilization, whereas only estimates are actually known, although these are refined in the iteration process. Second, a considerable volume of memory is needed, in addition to high computer speed, owing to the presence in the algorithm of matrices and vectors whose dimensions are governed by the sum of the number of grid nodes in the model and the number of unknown parameters.

The proposed economical algorithm makes it possible for us to rid ourselves of these shortcomings, since it provides us with estimates only of the unknown stochastic vector of the parameters being identified. As a result it becomes possible significantly to reduce the computer time required for the solution. Moreover, we eliminate the need to calculate the transition matrices which, in addition to the adaptability of the method to various problems, promotes the use of this method among adaptive categories [7]. For greater reliability in the derived estimates and so as to improve the quality of the computational algorithm significantly, we can make use of the so-called method of artificial filtration [8]. It involves the introduction of additional known model parameters into the measurement vector $\tilde{Y}$. In this case, all of the unknown parameters will enter the term in the right-hand side of the measurement equation Ah[Z], where Z is the vector formed by all of the identified and (or) corrected parameters, while the quality functional [9], minimized by the estimates obtained with aid of the adaptive filter, provision having been made for artificial filtration, will be written as follows:

$$J[\mathbf{Z}_k, \tilde{\mathbf{Y}}_k, j] = \| Ah(\hat{\mathbf{Z}}^{(j)}_{k/k}) - \tilde{\mathbf{Y}}_k \|^2_{R_k^{-1}} + \frac{1}{j} \| \mathbf{Z}_k - \hat{\mathbf{Z}}^{(j/j-1)}_{k/k} \|^2_{[P^{(s)}_{k-1/k-1}]^{-1}}. \tag{13}$$

Here j, s is the number of iterations, respectively, at the k + 1 and k time steps; R_k and $P_{k-1/k-1}$ are the covariational matrices of measurement and estimate error. In this case the estimate $\hat{Z}_{k/k}^{(j)}$, minimizing functional (13), is defined as the best. The latter indicates the nondisplacement ($M[Z_k - \hat{Z}_{k/k}^{(j)}] = 0$, where M[·] is the mathematical expectation) and minimum dispersion. Generally speaking, the estimate is obtained (with accuracy to the method of statistical linearization of the original mathematical model) and exhibits virtually no displacement. However, in the proposed method (and this is yet another one of its advantages) the original mathematical model requires no linearization. It may therefore be assumed, first of all, that the estimate is not displaced and that, second, the inadequacies of the mathematical model, introduced

by linearization, are eliminated. Moreover, a not unimportant positive quality of the method involves its stability relative to possible anomalies in the measurements.

The system of equations determining the computational algorithm has the following form:

$$\hat{\mathbf{Z}}^{(j)}_{k+1/k+1} = \tilde{\mathbf{Z}}^{(j/j-1)}_{k+1/k+1} + K^{(j)}_{k+1}\,[\tilde{\mathbf{Y}}_{k+1} - \hat{H}^{(j)}_{k+1}\hat{\mathbf{Z}}^{(j/j-1)}_{k+1/k+1}];\quad \hat{\mathbf{Z}}^{(j/j-1)}_{k+1/k+1} = \hat{\mathbf{Z}}^{(j-1)}_{k+1/k+1}; \tag{14}$$

$$K^{(j)}_{k+1} = P_{k/k}\,[\hat{H}^{(j)}_{k+1}]^{\mathrm{T}}\{\hat{H}^{(j)}_{k+1}P_{k/k}\,[\hat{H}^{(j)}_{k+1}]^{\mathrm{T}} + R_{k+1}\}^{-1}; \tag{15}$$

$$P_{k/k} = [I - K^{(s)}_{k-1}\hat{H}^{(s)}_{k-1}]\,P_{k-1/k-1}\,[I - K^{(s)}_{k-1}\hat{H}^{(s)}_{k-1}]^{\mathrm{T}} + K^{(s)}_{k-1}R_{k-1}\;[K^{(s)}_{k-1}]^{\mathrm{T}}, \tag{16}$$

where I is the unit matrix. The construction of the artificial measurement matrix $\hat{\mathbf{H}}_{k+1}$ is the most complex in algorithm (14)-(16), where it corresponds to the operator Ah in Eq. (12). The terms of this matrix represent partial derivatives of the "measured" parameters with respect to the estimated (identified, corrected)

$$\hat{H}^{(j)}_{k+1} = \left\{\frac{\partial \mathbf{Y}\,[\hat{\mathbf{Z}}^{(j-1)}_{k+1/k+1}]}{\partial \mathbf{Z}}\right\}^{(j)}_{k+1}. \tag{17}$$

We will not dwell here on calculations of the matrix H. Let us say only that for its construction by a numerical method it is necessary, several times in each iteration, to solve system of equations (2)-(11).

From among the general computational aspects involved in the utilization of algorithm (14)-(16) let us note that the poor convergence of the estimates $\mathbf{Z}_{k+1/k+1}{}^{(i)}$ may come about as a consequence of the nonsymmetricity of the covariational matrix of estimate errors (owing to the rounding off of results in the computer), or because of the sharp reduction in the norm, all the way to becoming comparable to the norm of the covariational measurement error matrix (as a consequence of the presence of the high-precision vector $\tilde{\mathbf{Y}}$. In order to improve convergence it is possible to use artificial means of averaging pairs of correlation moments symmetrical relative to the matrix diagonal and the "spurring" of the diagonal matrix elements $\mathbf{P_{k/k}}$ all the way to the initial quantities. Timely utilization of these methods enables us not only to improve convergence, but to maintain its velocity at an adequate level.

A positive aspect of this method is found also in the fact that it functions within the framework of the methods of stochastic modeling and unlike the determined numerical methods an accumulation of rounding errors is therefore not characteristic here, thus making it possible, when necessary, to utilize a limited-capacity computer.

In connection with the fact that it is only the single parameter $\mathbf{V_k}$ that is being identified and taking into consideration the "measurement" equation (12), let us simplify the recursion algorithm (14)-(17). Expressions (14) and (17) assume the form

$$\hat{V}^{(j)}_{k+1/k+1} = \hat{V}^{(j-1)}_{k+1/k+1} + K^{(j)}_{k+1}\,[T_{\mathrm{ph}} - \hat{H}^{(j)}_{k+1}\hat{V}^{(j-1)}_{k+1/k+1}]; \tag{18}$$

$$\hat{H}^{(j)}_{k+1} = \left\{\frac{\partial T_{\mathrm{ph}}(\check{V})}{\partial V}\right\}^{(j)}_{k+1}, \tag{19}$$

with the notation of Eqs. (15) and (16) remaining unchanged. The computational procedure of identifying the estimates of phase-separation boundary velocity of motion involves the successive utilization of formulas (18), (15), (19), and (16), in which all of the quantities ($\hat{V}$, $\tilde{T}_{\mathrm{ph}}$, $\hat{H}$, P, R, I) are scalar, i.e., the algorithm attains maximum efficiency with respect to both the required volume of memory and with respect to the time to solve the problem. In formula (18) T_{ph} represents the normal Gaussian sequence with the mathematical expectation $M[\tilde{T}_{\mathrm{ph}}] = \bar{T}_{\mathrm{ph}}$.

As a specific example we examined the optimization of the slag granulation process on a drum-type unit (see Fig. 1) where the drum diameter was R = 0.3 m and its length was B = 1.6 m. The wall of the drum with a thickness of Δ = 0.04 m was fabricated out of a copper-steel bimetal (the thickness of the copper was 0.03 mm and that of the steel was 0.01 m), and the copper surface is turned in the direction of the slag. For purposes of identifying $V(\tau)$ we used the following

TABLE 1. Thermal Conductivity of the Slag

T, °C	200	400	800	1200
λ, W/(m·K)	1,2	1,7	2,7	4,4

TABLE 2. Velocity of Crystallization Front Motion $V \cdot 10^4$ m/sec, with $\overline{T}_{ph} = 1100°C$

δ, m	Nodal number									
	7	8	9	10	11	12	13	14	15	16
0,001	4,3	3,2	3	2.75	2,6	2,2	2,0	1,9	1,9	1,8
0,0015	3,4	2,4	1,9	1,6	1,65	1,3	1,25	1,25	1,2	1,15
0,002	2,5	1,6	1,1	1	1,1	1,2	1,2	1,1	1,1	1,0
0,003	0,8	0,3	0,24	0,27	0,25	0,24	0,23	0,22	0,22	0,2

TABLE 3. Slag Aftercooling Time τ_2 and the Length ℓ of Zones I and II of the Granulation Process

$\delta \cdot 10^3$, m	1		1,5		2		3	
l_1, rad	$\pi R/2$	$\pi R/4$	$\pi R/2$	$\pi R/4$	$\pi R/2$	$\pi R/4$	$\pi R/2$	$\pi R/4$
τ_2, sec	0,9	1,125	1,4	1,75	2,1	2,625	4	5
l, m	0,647	0,573	0,605	0,538	0,589	0,53	0,504	0,487

copper-melt data provided by Gintsvetmet and the Krasnoyarsk Institute of Nonferrous Metals: $L = 273 \cdot 10^3$ J/kg; specific heat capacity $c_p = \{(155 + 0.5(T - 200))/T\} \cdot 10^3$ J/(kg·K); hardening temperature $T_{ph} = 1100°C$, $\partial T_{ph} \simeq 0.05 T_{ph}$; density of solid and liquid slag, respectively, $\rho_T = 3600$ kg/m^3, $\rho_s = 3000$ kg/m^3; initial temperature of the liquid slag $T_\ell = 1250°C$; temperature of the aftercooling of the slag skin $T_s = 700°C$. The thermal conductivity data for the slag can be found in Table 1. The effect of transition from water cooling of the drum to cooling in a boiling regime with a pressure of 0.6 MPa in the system (the boiling temperature $T_b = 164°C$) was accounted for by the change in the heat-transfer coefficient from 5000 to 15,000 W/(m^2·K) with an increase in the wall temperature from the cooling side to $(T_c + 20)$.

In order to develop the identification algorithm it becomes necessary to write the original mathematical model for the process being studied in finite-difference form [the approximation error is $O(h^2 + \Delta\tau)$]:

$$\left[\frac{\lambda_s(\hat{T}_i, \hat{T}_{i-1})}{h^2}\right]_{k+1/k+1}^{(j-1)} (T_{i-1})_{k+1}^{(j)} + \left[-\frac{\lambda_s(\hat{T}_i, \hat{T}_{i-1})}{h^2} - \frac{\lambda_s(\hat{T}_i, \hat{T}_{i+1})}{h^2} - \frac{c_{V_s}(\hat{T}_i)}{\Delta\tau}\right]_{k+1/k+1}^{(j-1)} (T_i)_{k+1}^{(j)} + \left[\frac{\lambda_s(\hat{T}_i, \hat{T}_{i+1})}{h^2}\right]_{k+1/k+1}^{(j-1)} \times (T_{i+1})_{k+1}^{(j)} = -\left[\frac{c_{V_s}(\hat{T}_i)}{\Delta\tau}\right]_{k+1/k+1}^{(j-1)} (\hat{T}_i)_{k/k}^{(s)}, \quad i = 7 \div 15; \tag{20}$$

$$\left[\frac{\lambda_d(\hat{T}_i, \hat{T}_{i-1})}{h_1^2}\right]_{k+1/k+1}^{(j-1)} (T_{i-1})_{k+1}^{(j)} + \left[-\frac{\lambda_d(\hat{T}_i, \hat{T}_{i-1})}{h_1^2} - \frac{\lambda_d(\hat{T}_i, \hat{T}_{i+1})}{h_1^2} - \frac{c_{V_d}(\hat{T}_i)}{\Delta\tau}\right]_{k+1/k+1}^{(j-1)} (T_i)_{k+1}^{(j)} + \left[\frac{\lambda_d(\hat{T}_i, \hat{T}_{i+1})}{h_1^2}\right]_{k+1/k+1}^{(j-1)} (T_{i+1})_{k+1}^{(j)} = -\left[\frac{c_{V_d}(\hat{T}_i)}{\Delta\tau}\right]_{k+1/k+1}^{(j-1)} (\hat{T}_i)_{k/k}^{(s)}, \quad i = 2 \div 5; \tag{21}$$

$$\left[\frac{c_{V_d}(\hat{T}_1) h_1}{2\Delta\tau} + \frac{\lambda_d(\hat{T}_1, \hat{T}_2)}{h_1} + \alpha_c\right]_{k+1/k+1}^{(j-1)} (T_1)_{k+1}^{(j)} - \left[\frac{\lambda_d(\hat{T}_1, \hat{T}_2]}{h_1}\right]_{k+1/k+1}^{(j-1)} \times (T_2)_{k+1}^{(j)} = \alpha_c T_c + \left[\frac{c_{V_d}(\hat{T}_1) h_1}{2\Delta\tau}\right]_{k+1/k+1}^{(j)} (\hat{T}_1)_k^{(s)}; \tag{22}$$

$$\left[\frac{\lambda_d(\hat{T}_6, \hat{T}_5)}{h_1} + \frac{\lambda_s(\hat{T}_6, \hat{T}_7)}{h} + \frac{c_{V_d}(\hat{T}_6) h_1}{2\Delta\tau} + \frac{c_{V_s}(\hat{T}_6) h}{2\Delta\tau}\right]_{k+1/k+1}^{(j-1)} (T_6)_{k+1}^{(j)} - \left[\frac{\lambda_d(\hat{T}_6, \hat{T}_5)}{h_1}\right]_{k+1/k+1}^{(j-1)} (T_5)_{k+1}^{(j)} - \left[\frac{\lambda_s(\hat{T}_6, \hat{T}_7)}{h}\right]_{k+1/k+1}^{(j-1)} (T_7)_{k+1}^{(j)} =$$

$$= \left[\frac{c_{V_d}(\hat{T}_6) h_1}{2\Delta\tau} + \frac{c_{V_s}(\hat{T}_6) h}{2\Delta\tau} \right]_{k+1/k+1}^{(j-1)} (\hat{T}_6)_k^{(s)}; \tag{23}$$

$$\left\{ \frac{\lambda_{s.\ell}(\hat{T}_{m+1}, \hat{T}_{m+2})}{h} + \frac{\lambda_{s.sol}(\hat{T}_{m+1}, \hat{T}_m)}{h} + \right.$$

$$\left. + \frac{[c_{V_{s.sol}}(\hat{T}_{m+1}) + c_{V_{s.\ell}}(\hat{T}_{m+1})] h}{2\Delta\tau} \right\}_{k+1/k+1}^{(j-1)} (T_{m+1})_{k+1}^{(j)} - \tag{24}$$

$$- \left[\frac{\lambda_{s.sol}(\hat{T}_{m+1}, \hat{T}_{m+2})}{h} \right]_{k+1/k+1}^{(j-1)} (T_{m+2})_{k+1}^{(j)} -$$

$$- \left[\frac{\lambda_{s.\ell}(\hat{T}_{m+1}, \hat{T}_m)}{h} \right]_{k+1/k+1}^{(j-1)} (T_m)_k^{(j)} +$$

$$+ \left\{ \frac{L}{N} [\rho_{s.sol}(\hat{T}_{m+1}) + \rho_{s.\ell}(\hat{T}_{m+1})]/2 \right\}_{k+1/k+1}^{(j-1)} V_k^{(j)} =$$

$$= \left\{ \frac{[c_{V_{s.sol}}(\hat{T}_{m+1}) + c_{V_{s.\ell}}(\hat{T}_{m+1})] h}{2\Delta\tau} \right\}_{k+1/k+1}^{(j-1)} (\hat{T}_{m+1})_k^{(s)},$$

(m + 1) changes from 7 to 15 in accordance with the movement of the crystallization front;

$$\left[\frac{c_{V_s}(\hat{T}_{16}, \hat{T}_{15}) h}{2\Delta\tau} + \frac{\lambda_s(\hat{T}_{16}, \hat{T}_{15})}{h} + \alpha_a \right]_{k+1/k+1}^{(j-1)} (T_{16})_{k+1}^{(j)} -$$

$$- \left[\frac{\lambda_s(\hat{T}_{16}, \hat{T}_{15})}{h} \right]_{k+1/k+1}^{(j-1)} (T_{15})_{k+1}^{(j)} = \alpha_a \bar{T}_a +$$

$$+ \left[\frac{c_{V_s}(\hat{T}_{16}) h}{2\Delta\tau} \right]_{k+1/k+1}^{(j-1)} (\hat{T}_{16})_k^{(s)} + \varepsilon C_0 \left\{ \left[\frac{(\hat{T}_{16})_k^{(s)}}{100} \right]^4 - \left(\frac{T_a}{100} \right)^4 \right\}, \tag{25}$$

$$l_1 < k\Delta\tau \leqslant l;$$

$$T_{16} = T_\ell, \quad 0 < k\Delta\tau \leqslant l_1. \tag{26}$$

In expressions (20)-(26) h = $\delta/10$, $h_1 = \Delta/5$, V = dx/dt is the unknown velocity of phase-separation boundary motion dependent on the location of the (m + 1) node closest to this boundary. The temperatures used in the calculations of the coefficients in the equations derived in the previous (j - 1)-th iteration of the (k + 1)-th time step after substitution of the estimates $\hat{V}_{k+1/k+1}^{(j-1)}$ into Eqs. (20)-(26) and their subsequent solution; s is the number of iterations in the k-th time step. The quantity V(τ) is identified in the first stage of problem solution, and it is decisive in the determination of the velocity W for drum rotation, since the process of hardening must be completed by the time the slag skin exits from the bath (zone I, Fig. 2).

At the very beginning of the first stage we solved the direct problem of heat conduction, i.e., for so long as the thickness of the solid slag phase does not exceed the magnitude of the step h(m + 1 $\geq$ 7). The program is compiled in a manner such that after its completion the identification algorithm (18), (15), (19), and (16) begins automatically to function, and its utilization makes it possible to obtain estimates for the velocity of crystallization-front motion. To calculate measurement matrix (19) we have to enhance system of equations (20)-(26) with the expression $\dot{V} = 0$ or in discrete form

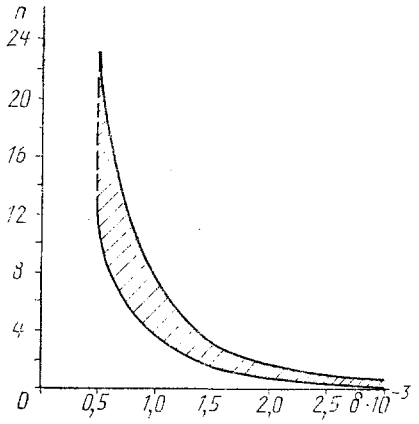

Fig. 4. Number of drum revolutions as a function of; flag skin thickness. n) rpm: δ, m.

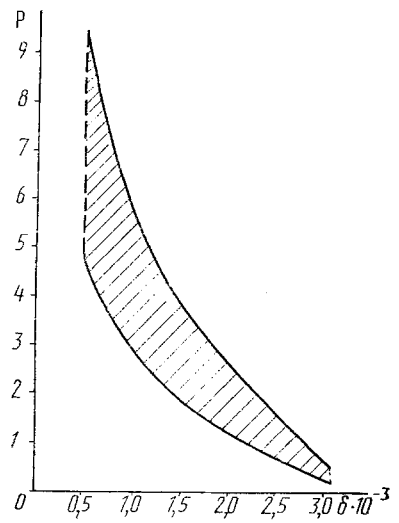

Fig. 5. Granulation installation productivity as a function of slag skin thickness. P, tons/h.

$V_{k+1} = V_k(V_{k+1}^{(j)} = V_{k+1}^{(j-1)})$ which is valid when the iteration filter is used [5]. The results from the identification of $V_k^{(j)}$ in dependence on the displacement of the phase-separation boundary (through nodes 7-15 when $T[x(\tau_0)] = T_6$ and $T[x(\tau_k)] = T_{16}$) and in dependence on the slag skin thickness δ can be seen in Table 2. Analysis of the results confirms the general trend toward reducing the velocity V_k as the thickness of the solid phase is increased, and this independent of the quantity δ. In our opinion, this is explained by the low thermal conductivity of the slags, exhibiting particular reduction for the solid phase. The stage is concluded at the instant that the cross section AB (Fig. 3) moves beyond the limits of the liquid-slag bath (at a distance ℓ_1 from the start of the crystallization process). Having determined V_k, it is easy to find the time τ_1 for the conclusion of the hardening process for all δ, and then to find the speed W of drum rotation. Indeed, as was noted earlier, the time for the displacement of the crystallization front through thickness δ is equal to the time required for the passage of any arbitrary point on the drum surface over the distance ℓ_1. Thus, $W = \ell/\tau_1$ (m/sec) or $n = W60/(2\pi R)$ (rpm). Since the quantity ℓ_1 (zone I, Fig. 2) for actual granulators varies within limits from 1/8 to 1/4 of the length of the circumference, the function $n = f(\delta)$ is shown in Fig. 4 in the form of an area whose boundaries correspond to the velocities W, calculated for extreme values of ℓ_1, equal to 1/4 and 1/8 of the drum circumference.

On completion of the first stage, when no liquid phase exists any longer ($m + 1 > 15$), and the surface temperature of the slag skin has reached $\bar{T}_{ph}$, that is when the second stage begins (the aftercooling of the slag to T_{af}, at which its foliation starts). The range $\bar{T}_{ph} - T_{af}$ determines the level of slag-heat utilization. The calculations in the transition from the first stage to the second are interrupted. The program automatically accomplishes the transition to the direct heat-conduction problem which is solved until the temperature at the hottest point of the skin surface reaches T_{af}. With this

the second stage is concluded, and together with this conclusion the actual solution of the heat-conduction problem. We then calculate the time for the aftercooling of these slag skins (the duration τ_2 of the second stage) according to which, as a result of the solution of the problem in the first stage, we have the speed of drum rotation, it is not difficult to determine that part of the circumference ℓ (Fig. 3) at which the slag hardens to the required state. The results from the calculations of $\ell = \ell_1 + W\tau_2$ in combination with the values of ℓ_1 and τ_2 can be found in Table 3.

The foliation of the slag usually occurs at a specific distance from the starting point of the process. This distance ℓ_c is equal to the length of zones I and II and is independent of the overall length ℓ of the first and second stages, with compulsory satisfaction of the condition $\ell \leq \ell_c$. Since all of the values of ℓ are less than 3/4 of the drum circumference (Table 3), it is correct to choose $\ell_c = 3\pi R/2$.

The resulting data regarding the hardening and cooling of the slag of a specific composition make it possible to estimate the productivity P of the installation being studied:

$$P = (ml_cB\rho \cdot 10^3)\,\delta n \cdot 60, \quad [\text{tons/h}], \tag{27}$$

where m = 2 is the number of drums; $\ell_c = 3\pi R/2$; B = 1.6 m; $\rho = 3000$ kg/m^3. Since the function $n = f(\delta)$ is shown in the form of an area (Fig. 4) the function $P = f_1(\delta)$ will have an analogous form (Fig. 5). Analysis of the latter shows that an increase in the thickness of the slag skin above 3 mm leads to a sharp reduction in the operational productivity of the granulator and confirms the practical impossibility of producing a skin with a thickness greater than 3-4 mm. However, the reduction of δ leads to a considerable increase in P as a result of an equally intensive increase in n (see Fig. 4). However, reduction in the skin thickness to $\delta \leq 0.0005$ m by raising the number of revolutions is not expedient, since this may lead to splattering of the slag melt. Any further increase in productivity becomes possible only by increasing the area of the cooling surface.

The studies conducted for the more complex two-drum granulator are valid also for other granulator types which utilize the slag heap with rotational or translational forms of crystallization surface motion, since $\delta \ll \ell$ and the processes of heat exchange are invariant for all types of devices, and the differences in the functions $P = f_1(\delta)$ are only quantitative in nature. By utilizing the results [expression (27), Fig. 5] we can calculate the geometric parameters of the projected dry-granulation installation for a specific metallurgical aggregate yielding a known output of slag.

NOTATION

T, temperature; λ, thermal conductivity; c_V, specific volumetric heat capacity; R, drum radius; Δ, thickness of drum wall; δ, thickness of slag skin; $V(\tau)$, linear hardening rate; α, heat transfer coefficient; ε, emissivity; L, latent heat of crystallization; J, quality functional; Z, identified parameters; Y, measurements; j, s, number of iterations at the (k + 1)-th and k-th time steps; R_k, $P_{k/k}$, covariational matrices; M[·], mathematical expectation; $\hat{Z}_{k+1/k+1}^{(j)}$, estimate of identified parameter; H_k, measurement matrix; K, weighted matrix; T_{af}, aftercooling temperature; $\Delta\tau$, h, time and space steps; (m + 1), number of the node on the phase transition boundary; W, speed of drum rotation; P, productivity. Subscripts: ph, phase transition; s, slag; d, drum.

LITERATURE CITED

1. J. Medich, *Statistically Optimum Linear Estimates and Control* [Russian translation], Moscow (1973).
2. É. I. Guiko (ed.), *Drum-Type Freezing Apparatus* [in Russian], Leningrad (1986).
3. V. M. Case, *Convective Heat and Mass Exchange* [Russian translation], Moscow (1972).
4. V. V. Sobolev, F. M. Chernomurov, and V. V. Mechev, *Izv. vuzov. Tsvetnaya metallurgiya*, No. 3, 62-65 (1984).
5. Yu. M. Matsevitiyi and A. V. Multanovskii, *Identification in Heat-Conduction Problems* [in Russian], Kiev (1982).
6. Yu. M. Matsevityi and A. V. Multanovskii, *Inzh.-Fiz. Zh.*, 35, No. 5, 916-923 (1978).
7. K. T. Leondes (ed.), *Filtration and Stochastic Control in Dynamic Systems* [in Russian], Moscow (1980).
8. J. Kucas (ed.), *Heat Exchange and the Thermal Regime in Spacecraft* [in Russian], Moscow (1974).
9. Yu. M. Matsevityi and A. V. Multanovskii, *Problems in Nonlinear Electrical Engineering* [in Russian], Kiev (1981), pp. 114-117.